

## **Binuclear cobalt(II) and two-dimensional manganese(II) coordination compounds self-assembled by mixed bipyridine-tetracarboxylate with single-ion magnet properties**

Dong-Qing Wu, <sup>\*a</sup> Kusum Kumari, <sup>c</sup> Yi Wan, <sup>b</sup> Xueling Gao, <sup>a</sup> Mengxi Guo, <sup>a</sup> Genyan Liu, <sup>d</sup> Dong Shao, <sup>\*b</sup> Bin Zhai <sup>a</sup> and Saurabh Kumar Singh <sup>\*c</sup>

<sup>a</sup> Engineering Research Center of Photoelectric Functional Material, School of Chemistry and Chemical Engineering, Shangqiu Normal University, Shangqiu 476000, P. R. China.

<sup>b</sup> Hubei Key Laboratory of Processing and Application of Catalytic Materials, College of Chemistry and Chemical Engineering, Huanggang Normal University, Huanggang 438000, P. R. China

<sup>c</sup> Department of Chemistry, Indian Institute of Technology Hyderabad, Kandi-502285, Sangareddy, Telangana, India

<sup>d</sup> *Hubei Key Laboratory of Novel Reactor and Green Chemical Technology, Wuhan Institute of Technology, Wuhan 430205, P. R. China*

Email: iamwudongqing@163.com; shaodong@nju.edu.cn; sksingh@chy.iith.ac.in

## Table of Contents

EXPERIMENTAL SECTION .....	4
<b>Figure S1.</b> Comparison of the experimental and simulated PXRD patterns of <b>1</b> .....	6
<b>Figure S2.</b> Comparison of the experimental and simulated PXRD patterns of <b>2</b> .....	6
<b>Figure S3.</b> The TGA curve of complex <b>1</b> .....	7
<b>Figure S4.</b> The TGA curve of complex <b>2</b> .....	7
<b>Figure S5.</b> The asymmetric unit of complex <b>1</b> .....	8
<b>Figure S6.</b> The asymmetric unit of complex <b>2</b> .....	8
Table S1. Selected bond lengths (Å) in <b>1</b> . ....	9
Table S2. Selected bond angles (Å) in <b>1</b> .....	9
Table S3. Selected bond lengths (Å) in <b>2</b> . ....	10
Table S4. Selected bond angles (Å) in <b>2</b> .....	10
Table S5. Continuous Shape Measure (CSM) analysis for <b>1</b> and <b>2</b> .....	11
<b>Figure S7.</b> the magnetization curves for <b>1</b> measured at 2, 3, 4, and 5 K. The green solid lines represent the best fits by PHI. ....	12
<b>Figure S8.</b> the magnetization curves for <b>2</b> measured at 2, 3, 4, and 5 K. The green solid lines represent the best fits by PHI. ....	12
<b>Figure S9.</b> Frequency dependence of the ac susceptibilities measured under zero dc field at 1.8 K for <b>1</b> . ....	13
<b>Figure S10.</b> Frequency dependence of the ac susceptibilities measured under zero dc field at 1.8 K for <b>2</b> . ....	13
<b>Figure S11.</b> Temperature dependence of the in-phase ( $\chi'$ ) and out-of-phase ( $\chi''$ ) ac susceptibilities measured under 1 kOe dc field for <b>1</b> .....	14
<b>Figure S12.</b> Temperature dependence of the in-phase ( $\chi'$ ) and out-of-phase ( $\chi''$ ) ac susceptibilities measured under 1 kOe dc field for <b>2</b> .....	15
<b>Figure S13.</b> Cole-Cole plots of <b>1</b> obtained from 1 kOe dc field. The solid lines represent the best fits according to the generalized Debye model. ....	16
<b>Figure S14.</b> Cole-Cole plots of <b>2</b> obtained from 1 kOe dc field. The solid lines represent the best fits according to the generalized Debye model. ....	16
Table S6. Relaxation fitting parameters from the least-square fitting of the Cole-Cole plots of <b>1</b> under 1 kOe dc field according to the generalized Debye model.....	17
Table S7. Relaxation fitting parameters from the least-square fitting of the Cole-Cole plots of <b>2</b> under 1 kOe dc field according to the generalized Debye model.....	18
Table S8. CASSCF/NEVPT2 computed 10 spin-free quartet (red) and 40 spin-free doublet (blue) states along the spin-orbit states for Co@1 in complex <b>1</b> . All values are reported here in $\text{cm}^{-1}$ .....	19

Table S9. CASSCF/NEVPT2 computed 10 spin-free quartet (red) and 40 spin-free doublet (blue) states along the spin-orbit states for Co@2 in complex 1. All values are reported here in $\text{cm}^{-1}$ .....	20
Table S10. CASSCF (7,5) + NEVPT2 computed Spin – Hamiltonian parameter ( $g$ , $D$ , $ E/D $ ) along with listed state – by – state contribution to the $D$ values for both centre Co@1 and Co@2 in complex 1. ....	21
Table S11: NEVPT2 computed spin-Hamiltonian parameters along with experimental studies obtained from PHI fitting for Cobalt centres in Complex 1. ....	22
Table S12. AILFT-derived ligand field parameters computed at CASSCF (in parentheses) and NEVPT2 level of theory for both centre Co@1 and Co@2 in complex 1 along with free Co(II) ion. The values of $B$ , $C$ , $\xi$ parameters are provided in units of $\text{cm}^{-1}$ .....	22
Figure S15. <i>Ab initio</i> ligand field theory (AILFT) computed d-orbital ordering for cobalt Co@1 (left) and Co@2 (right) in complex 1. Color code: Co (cyan), N (blue), O (red), C (grey) and H (white). .....	23
.....	.. 24
Figure S16. NEVPT2 computed $g$ -tensor orientation in complex 1. Color code: Co (cyan), N (blue), O (red), C (grey). Hydrogen atoms are omitted for clarity.....	24
Figure S17. Experimental and <i>ab initio</i> computed magnetic susceptibility data of complex 1. ....	25
Figure S18. <i>Ab initio</i> computed magnetization curves for complex 1 at 2K, 3K and 5K.....	25
Figure S19. BS-DFT computed spin-density plot of ( $S = 3$ ) ground state of 1. The positive and negative spin densities are represented by purple and green colour, respectively. The iso-density surface represented here corresponds to a value of $0.005410 e^- / \text{bohr}^3$ .....	26
Table S13. BS-DFT computed energies of high-spin and broken-symmetry of complex 1 using $H = -2JS_1S_2$ formalism. ....	27
Table S14. Comparison of the lattice parameters of complex 2 with the experimentally reported structure. ....	28
Figure S20. a) $1 \times 1 \times 1$ supercell of complex 2 showing the Charge Density plot b) Spin density plot of complex 2 showing the electron density on each Mn(II) centres c) ELF plot for complex 2 d) Density of States plot for complex 2.....	29
Table S15. CASSCF (7,5) + NEVPT2 computed Spin – Hamiltonian parameter ( $g$ , $D$ , $ E/D $ ) along with listed state – by – state contribution to the $D$ value for Mn (II) center in complex 2m. ....	30
Figure S21. a) NEVPT2 computed $D$ -tensor orientation and b) DFT computed $D$ -tensor orientation in a mononuclear model complex 2m. Color code: Mn (pink), N (blue), O (red), C (grey) and H (white). ....	31
Figure S22. <i>Ab initio</i> ligand field theory (AILFT) computed d-orbital ordering for complex 2m. Color code: Mn (pink), N (blue), O (red), C (grey) and H (white). ....	33
Figure S23. Experimental and <i>Ab initio</i> computed magnetic susceptibility plots for complex 2m. The blue and red lines correspond to CASSCF and NEVPT2 computed data, respectively. ....	34
Table S17. CASSCF/NEVPT2 computed 1 spin-free sextet, 24 quartets and 75 doublets spin-free states along the spin-orbit states for Co centre1 in complex 2m. All values are reported here in $\text{cm}^{-1}$ . ....	35
<b>References</b> .....	36

## EXPERIMENTAL SECTION

### Physical measurements

Elemental analyses of C, H, and N were performed at an Elementar Vario MICRO analyzer. Infrared spectra were obtained in the range of 600–4000  $\text{cm}^{-1}$  on a Bruker tensor II spectrometer. Variable-temperature powder X-ray diffraction data (PXRD) were recorded on a Bruker D8 Advance diffractometer with Cu  $K\alpha$  X-ray source ( $\lambda = 1.54056 \text{ \AA}$ ) operated at 40 kV and 40 mA between 5 and 35° ( $2\theta$ ). Simulated PXRD patterns were obtained from the Mercury software. Thermal gravimetric analysis (TGA) was carried out on freshly filtered crystals using the Mettler Toledo TGA2 instrument in an insert Ar atmosphere over a temperature range of 27–700 °C with a heating rate of 10 °C/min.

### Magnetic measurements

Direct current (dc) magnetic susceptibility from 2 to 300 K with applied 1000 Oe dc field were performed using a Quantum Design SQUID VSM magnetometer on the crushed single crystals sample of **1**. Alternative current (ac) magnetic susceptibility data were collected in a zero-dc field or an applied 1000 Oe dc fields in the temperature range of 2-8 K, under an ac field of 2 Oe, oscillating at frequencies in the range of 1-1000 Hz. All magnetic data were corrected for the diamagnetic contributions of the sample holder and of core diamagnetism of the sample using Pascal's constants.

## X-ray Crystallography

Single crystal X-ray diffraction data were collected on a Bruker D8 QUEST diffractometer with a PHOTON III area detector (Mo-K $\alpha$  radiation,  $\lambda = 0.71073 \text{ \AA}$ , Bruker *lus* 3.0) at room temperature. Crystals were mounted on a CryoLoop (Hampton Research) with Paratone-N (Hampton Research) as cryoprotectant and then flash frozen in a nitrogen-gas stream at 120 K. The APEX III program was used to determine the unit cell parameters and for data collection. The data were integrated and corrected for Lorentz and polarization effects using SAINT.<sup>S1</sup> Absorption corrections were applied with SADABS.<sup>S2</sup> The structures were solved by direct methods and refined by full-matrix least-squares method on *F*<sup>2</sup> using the SHELXTL<sup>S3</sup> crystallographic software package integrated in Olex 2.<sup>S4</sup> All the non-hydrogen atoms were refined anisotropically. Hydrogen atoms of the organic ligands were refined as riding on the corresponding non-hydrogen atoms. CCDC 2274608 and 2274609 are the supplementary crystallographic data for this paper. They can be obtained freely from the Cambridge Crystallographic Data Centre via [www.ccdc.cam.ac.uk/data\\_request/cif](http://www.ccdc.cam.ac.uk/data_request/cif).

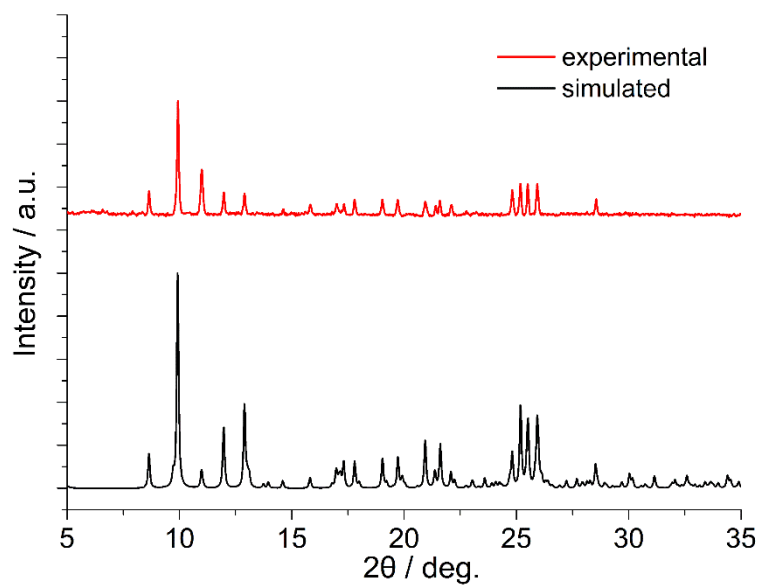


**Figure S1.** Comparison of the experimental and simulated PXRD patterns of **1**.

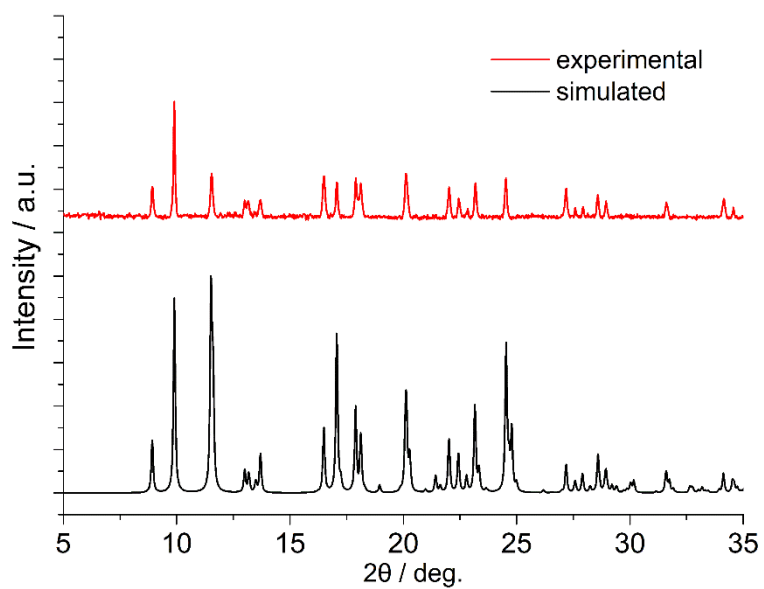


**Figure S2.** Comparison of the experimental and simulated PXRD patterns of **2**.

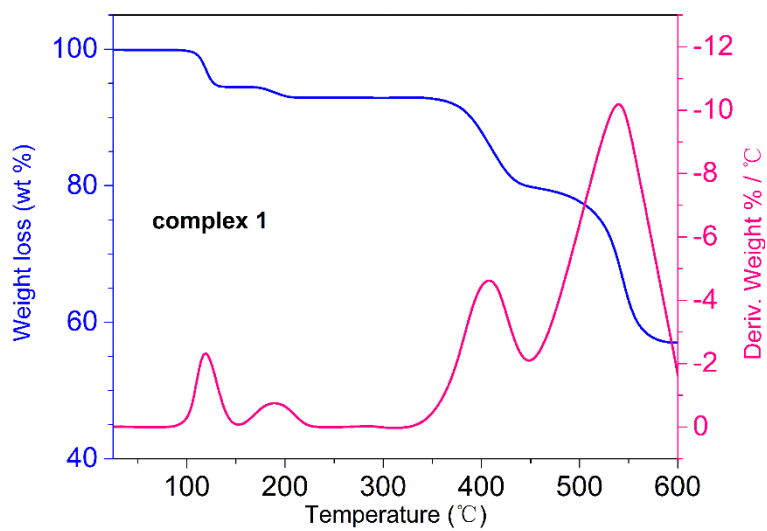


**Figure S3.** The TGA curve of complex 1

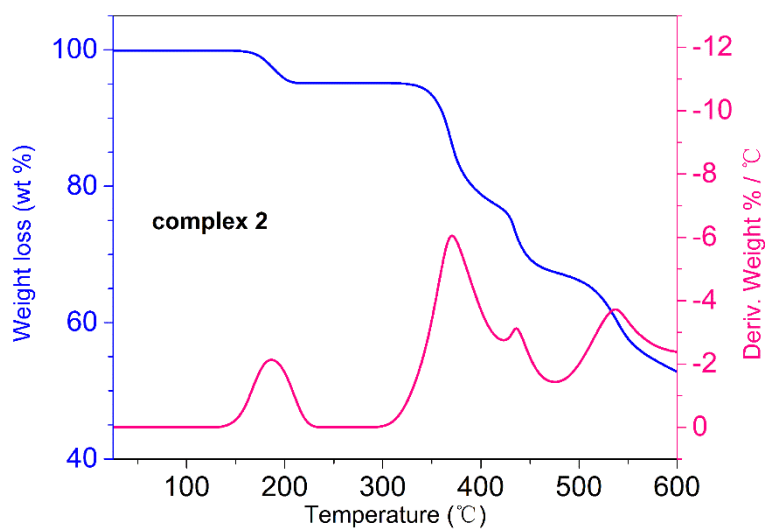


**Figure S4.** The TGA curve of complex 2.

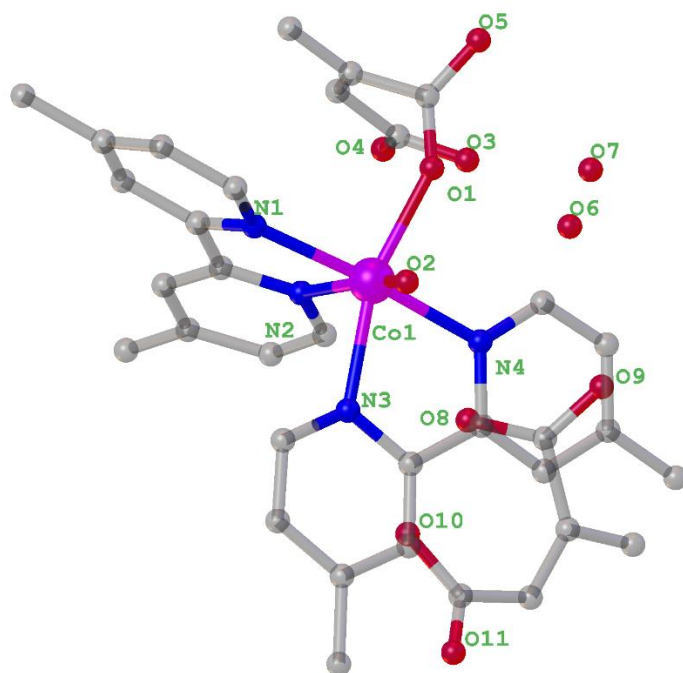


**Figure S5.** The asymmetric unit of complex 1.

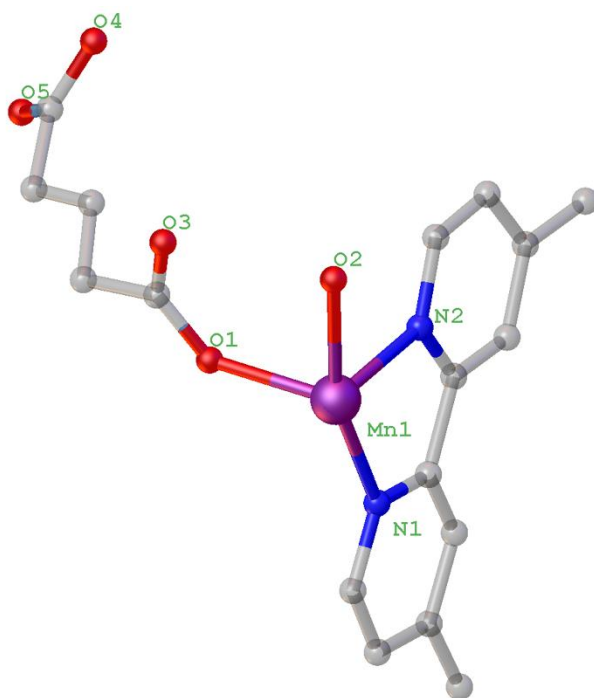


**Figure S6.** The asymmetric unit of complex 2.



**Table S1.** Selected bond lengths (Å) in **1**.

Co1-O1	2.0619(15)
Co1-O2	2.0871(15)
Co1-N1	2.1386(17)
Co1-N2	2.1543(18)
Co1-N3	2.1535(18)
Co1-N4	2.1164(17)
Co-N/O <sub>average</sub>	2.1186
Symmetry operation: <sup>1</sup> 1-X,1-Y,-Z; <sup>2</sup> -X,-Y,1-Z	

**Table S2.** Selected bond angles (°) in **1**.

O1-Co1-O2	87.30(6)
O1-Co1-N1	93.89(6)
O1-Co1-N2	105.43(6)
O1-Co1-N3	161.70(6)
O2-Co1-N2	162.51(7)
N1-Co1-N3	101.72(7)
N4-Co1-N1	172.56(7)
N4-Co1-N2	96.51(7)
N4-Co1-N3	75.71(7)
O2-Co1-N3	82.94(6)
O2-Co1-N4	95.44(6)
Symmetry operation: <sup>1</sup> 1-X,1-Y,-Z; <sup>2</sup> -X,-Y,1-Z	

**Table S3.** Selected bond lengths (Å) in **2**.

Mn1-O1	2.0652(13)
Mn1-O2	2.1479(15)
Mn1-O4 <sup>1</sup>	2.2839(12)
Mn1-O5 <sup>1</sup>	2.2426(13)
Mn1-N1	2.2605(16)
Mn1-N2	2.2538(16)
Mn-N/O <sub>average</sub>	2.209
Symmetry operation: <sup>1</sup> 1/2+X,3/2-Y,1/2+Z; <sup>2</sup> 1-X,2-Y,-Z	

**Table S4.** Selected bond angles (Å) in **2**.

O1-Mn1-O2	87.02(6)
O1-Mn1-O4 <sup>1</sup>	94.25(5)
O1-Mn1-O5 <sup>1</sup>	148.59(5)
O1-Mn1-N1	101.31(6)
O1-Mn1-N2	97.17(6)
O2-Mn1-N1	161.85(7)
O2-Mn1-N2	90.94(7)
N1-Mn1-O4 <sup>1</sup>	88.43(5)
N2-Mn1-N4 <sup>1</sup>	159.05(6)
N2-Mn1-N1	72.16(6)
O2-Mn1-O5 <sup>1</sup>	88.26(6)
Symmetry operation: <sup>1</sup> 1/2+X,3/2-Y,1/2+Z; <sup>2</sup> 1-X,2-Y,-Z	

**Table S5.** Continuous Shape Measure (CSM) analysis for **1** and **2**.

Compound, Metal center	CSM parameters*					Determined coordination geometry
	six-coordinated coordination sphere					
	HP-6	PPY-6	OC-6	TPR-6	JPPY-6	
<b>1_Co</b>	29.373	22.162	<b>1.883</b>	9.902	25.501	OC-6
<b>2_Mn</b>	30.134	16.162	<b>5.061</b>	8.843	19.788	

\* CSM parameters for six-coordinated complexes: <sup>5</sup>

HP-6 the parameter related to the hexagon ( $D_{6h}$ )

PPY-6 the parameter related to the pentagonal pyramid ( $C_{5v}$ )

OC-6 the parameter related to the octahedron ( $O_h$ )

TPR-6 the parameter related to the trigonal prism ( $D_{3h}$ )

JPPY-6 the parameter related to the Johnson pentagonal pyramid ( $C_{5v}$ )

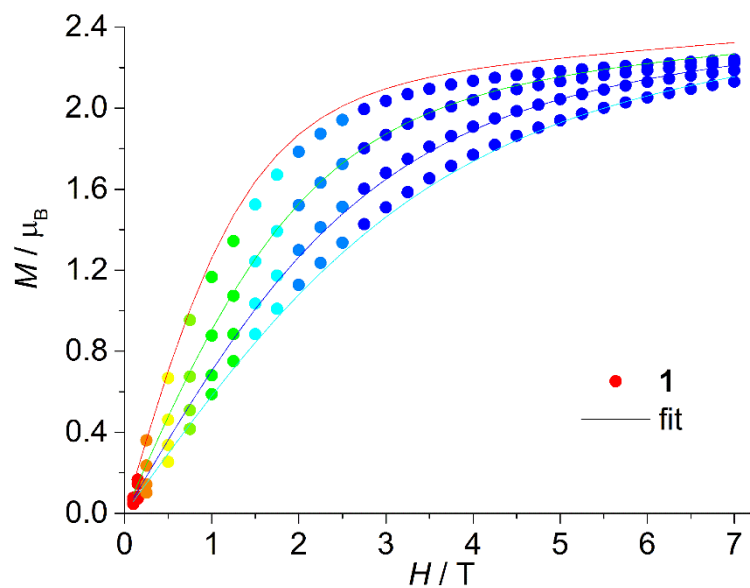


**Figure S7.** the magnetization curves for **1** measured at 2, 3, 4, and 5 K. The green solid lines represent the best fits by PHI.

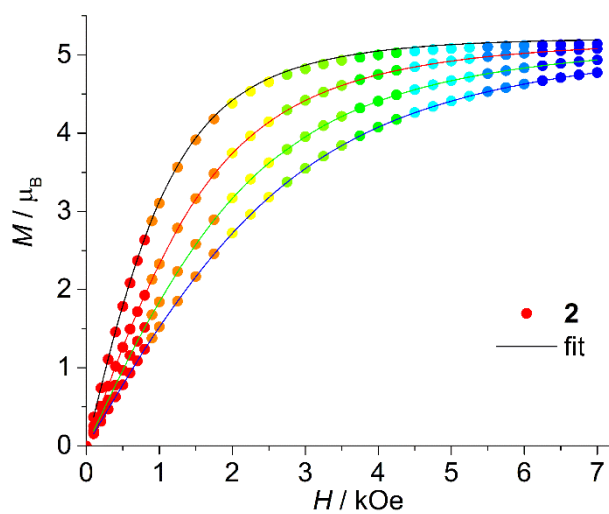


**Figure S8.** the magnetization curves for **2** measured at 2, 3, 4, and 5 K. The green solid lines represent the best fits by PHI.

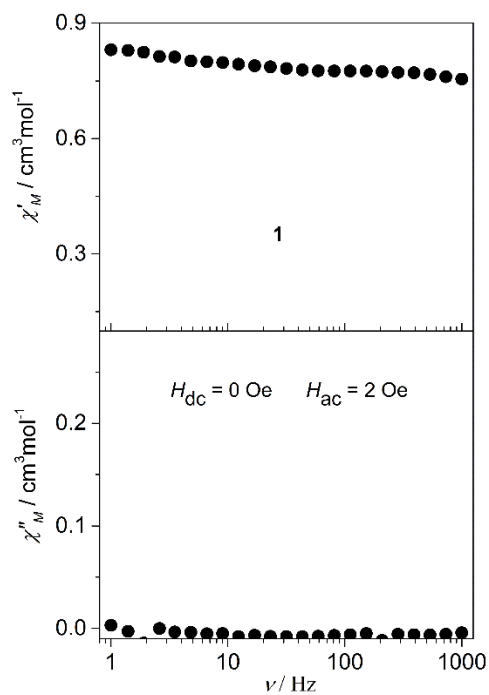


**Figure S9.** Frequency dependence of the ac susceptibilities measured under zero dc field at 1.8 K for **1**.

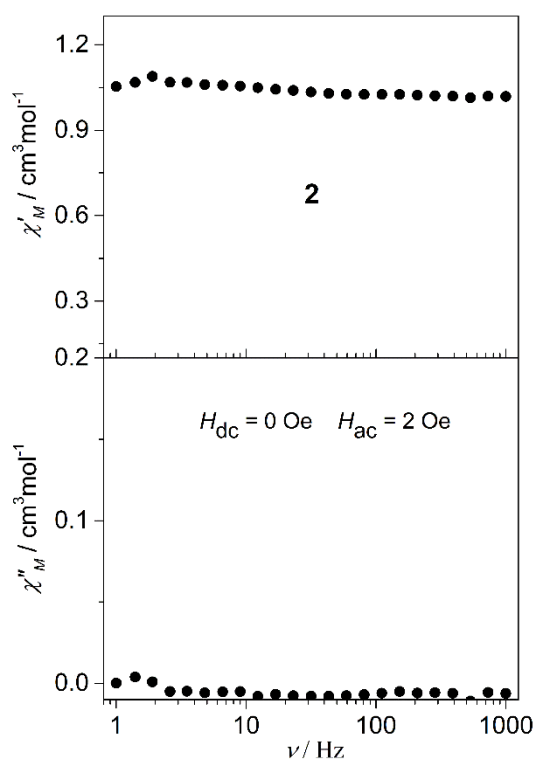


**Figure S10.** Frequency dependence of the ac susceptibilities measured under zero dc field at 1.8 K for **2**.

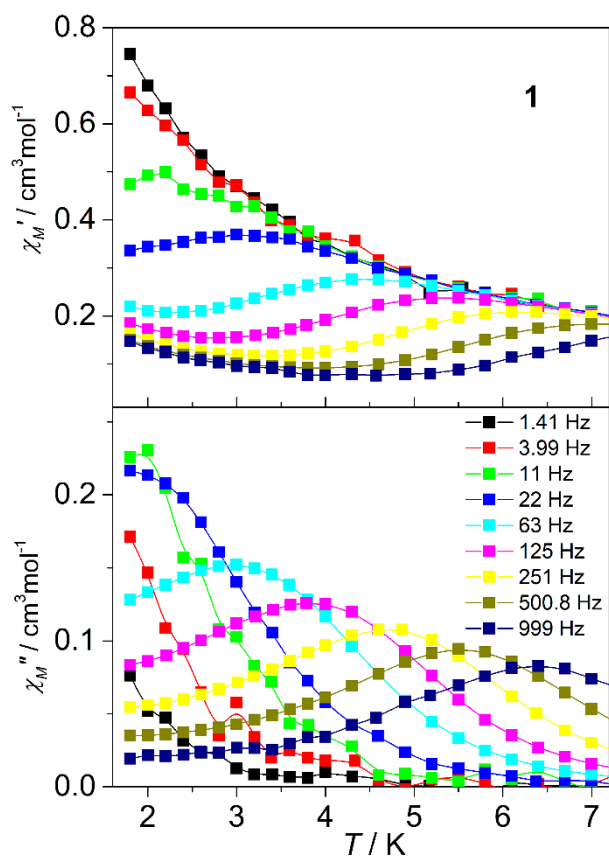


**Figure S11.** Temperature dependence of the in-phase ( $\chi'$ ) and out-of-phase ( $\chi''$ ) ac susceptibilities measured under 1 kOe dc field for **1**.

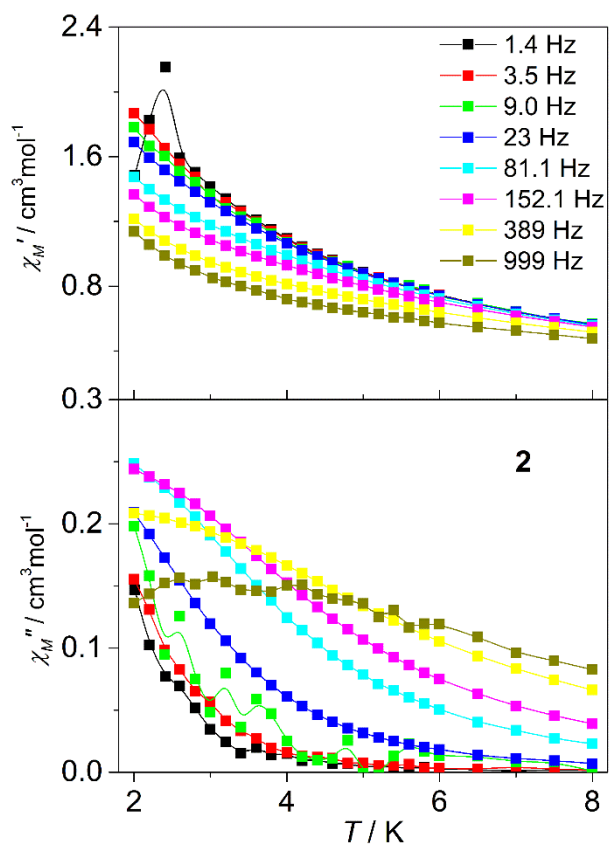


**Figure S12.** Temperature dependence of the in-phase ( $\chi'$ ) and out-of-phase ( $\chi''$ ) ac susceptibilities measured under 1 kOe dc field for **2**.

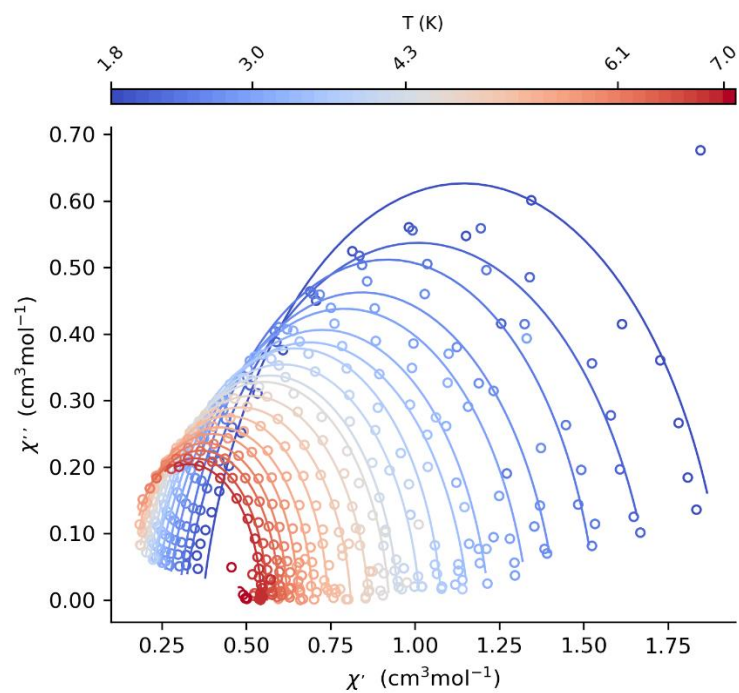


**Figure S13.** Cole-Cole plots of **1** obtained from 1 kOe dc field. The solid lines represent the best fits according to the generalized Debye model.

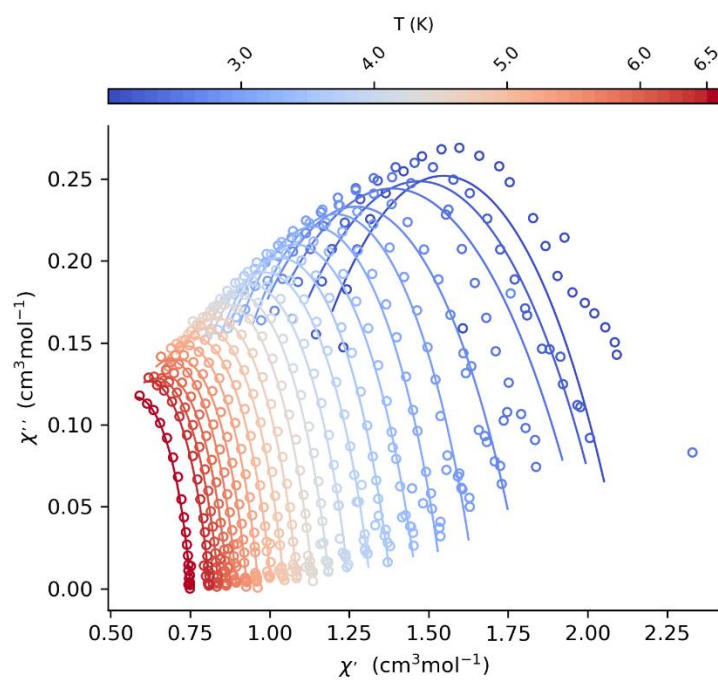


**Figure S14.** Cole-Cole plots of **2** obtained from 1 kOe dc field. The solid lines represent the best fits according to the generalized Debye model.



**Table S6.** Relaxation fitting parameters from the least-square fitting of the Cole-Cole plots of **1** under 1 kOe dc field according to the generalized Debye model.

T / K	$\tau$ / s	$\chi_S$ / cm <sup>3</sup> mol <sup>-1</sup> K	$\chi_T$ / cm <sup>3</sup> mol <sup>-1</sup> K	$\alpha$
2.00014	0.01036	0.10493	0.56997	0.16254
2.20019	0.00786	0.10024	0.5141	0.11999
2.4002	0.00673	0.08898	0.47451	0.13896
2.59985	0.00573	0.08287	0.44653	0.13661
2.79978	0.00452	0.07739	0.40775	0.12359
3.00075	0.00384	0.07186	0.38745	0.12474
3.20021	0.00307	0.07211	0.36064	0.08327
3.39952	0.00259	0.06729	0.33909	0.087
3.59898	0.00211	0.06308	0.31782	0.07656
3.79954	0.00183	0.05996	0.30881	0.08028
3.99876	0.0015	0.05548	0.28861	0.08085
4.30148	0.00117	0.05285	0.27087	0.07495
4.59933	8.7642E-4	0.05208	0.24802	0.03672
4.89655	6.66561E-4	0.04729	0.23311	0.04291
5.19703	5.19558E-4	0.04812	0.2181	0.0114
5.49837	4.0265E-4	0.04605	0.20755	0.01467
5.79975	3.18965E-4	0.04436	0.19984	0.02192
6.10102	2.47144E-4	0.04503	0.18767	7.47837E-4
6.3974	1.91638E-4	0.03913	0.18221	0.03018

**Table S7.** Relaxation fitting parameters from the least-square fitting of the Cole-Cole plots of **2** under 1 kOe dc filed according to the generalized Debye model.

T / K	$\tau$ / s	$\chi_S / \text{cm}^3\text{mol}^{-1}\text{K}$	$\chi_T / \text{cm}^3\text{mol}^{-1}\text{K}$	$\alpha$
2.00115	0.00156	0.97251	2.11943	0.47288
2.20085	0.00156	0.85449	2.08464	0.51081
2.40065	0.00136	0.74886	2.02063	0.53306
2.60028	0.00102	0.74506	1.79693	0.46859
2.80014	9.38532E-4	0.76658	1.6483	0.391
3.00126	8.02838E-4	0.73168	1.54464	0.366
3.20009	7.11073E-4	0.6966	1.46423	0.36238
3.40012	6.55495E-4	0.68557	1.38263	0.33179
3.60009	5.78639E-4	0.65167	1.31877	0.33207
3.80009	5.14847E-4	0.63105	1.25059	0.3131
4.0001	4.46872E-4	0.60335	1.19016	0.29977
4.20005	4.00411E-4	0.58011	1.13829	0.29145
4.40001	3.73458E-4	0.56865	1.08903	0.27881
4.6	3.41087E-4	0.54983	1.04625	0.27421
4.80001	3.02145E-4	0.52387	1.00607	0.27902
4.99998	2.78763E-4	0.51016	0.96512	0.265
5.19999	2.66829E-4	0.50576	0.92866	0.2555
5.39996	2.3047E-4	0.47322	0.89629	0.2582
5.60025	2.30329E-4	0.47635	0.86835	0.2559
5.79993	2.04392E-4	0.45114	0.83982	0.25664
5.99999	1.83921E-4	0.43148	0.81034	0.25017
6.49992	1.60416E-4	0.40725	0.75119	0.24038

**Table S8.** CASSCF/NEVPT2 computed 10 spin-free quartet (red) and 40 spin-free doublet (blue) states along the spin-orbit states for Co@1 in complex 1. All values are reported here in cm<sup>-1</sup>

Co@1							
SPIN-FREE STATES				SPIN-ORBIT STATES			
CASSCF		NEVPT2		CASSCF		NEVPT2	
0	36711.5	0	37422.6	0.0	31019.4	0.0	29474.4
484.2	36859.6	713	37515	174.5	32595.5	136.9	29703.8
1128.5	37062.1	1461.3	37573.1	677.6	32895.8	845.3	30396.5
7024.2	47076.1	9153.6	40953.4	973.5	35421.7	1091.1	31777.1
7420.3	47420.3	9692.1	41408.8	1463.2	35666.3	1718.5	32149.1
8142.7	47871	10593.9	42004.6	1577.8	35900.4	1831.6	34759.0
15624.5	48293.6	19984.1	43552.1	7317.9	36406.9	9196.1	34939.2
23700.1	49048.8	21889.2	44550.8	7371.4	36979.2	9374.1	35312.0
24177.3	49073.1	22410.4	44624.3	7718.2	37048.6	9416.8	36214.5
25280.4	49596.9	22410.4	44652.5	7782.2	37265.6	9909.3	37017.8
13855.5	72259.8	23750.8	63454.1	7782.2	37756.7	9909.3	37627.6
14981.5	72683.1	8934.3	64197.3	8438.7	47303.4	9982.0	37765.5
19832.3	73352.5	10439.2	64770	8528.9	47794.9	10709.9	38215.4
20081.1	73853.1	17509.9	65293	14164.5	48272.5	10815.4	41150.9
20111.6		17912.7		15287.7	48624.9	10903.2	41717.3
20345.6		18087.9		15977.6	49275.3	17726.4	42340.5
20940.2		18269.4		15982.0	49560.8	17991.4	43823.5
21119.2		19151.8		20060.0	49962.9	18416.7	44730.1
25447.4		19549		20167.6	72593.2	18624.2	44942.9
25827.3		22172.1		20566.2	73048.4	19463.8	45036.5
26157.4		22439.3		20779.0	73708.4	19827.1	63742.1
26305.1		22727.3		21351.7	74172.6	20290.0	64488.3
28945.9		25786.1		21579.2	74592.5	20290.0	65077.9
29248.4		27704.5		21579.2	31019.4	20357.7	65569.8
29820.2		27836.7		23832.0		21608.0	66123.8
30111.5		27836.7		23897.5		21870.9	
30211.4		29056.4		24295.7		22129.8	
30696.5		29191.7		24448.8		22451.6	
32227.5		29397.2		25237.1		22644.4	
32513.7		30141		25519.8		23113.7	
35216.4		31471.9		25658.1		23422.0	
35465.2		31835.5		26462.5		24164.9	
35640.5		34622.9		26722.0		24302.5	
36069.3		34740.9		27115.1		26113.1	
36237.8		34976.7		29286.4		27944.4	
		35844.1		29687.3		28248.9	
		36554.4		30160.9		29325.5	

**Table S9.** CASSCF/NEVPT2 computed 10 spin-free quartet (red) and 40 spin-free doublet (blue) states along the spin-orbit states for Co@2 in complex 1. All values are reported here in cm<sup>-1</sup>

Co@2							
SPIN-FREE STATES				SPIN-ORBIT STATES			
CASSCF		NEVPT2		CASSCF		NEVPT2	
0	36950.6	0	37590.3	0	30614.5	0	29677.8
502.6	37148.9	728.8	37737.4	169.5	31116.0	133.2	30533.9
1208.6	47116.6	1569.5	41007.8	695.4	32603.7	865.2	31797.6
7118.6	47451.3	9293.4	41473.6	978.2	32965.6	1097.6	32262.5
7362	47910.2	9611.9	42078.1	1530.9	35454.6	1816.2	34823.7
8241.4	48342.3	10735.6	43617.3	1638.8	35659.9	1920.9	34975.3
15674.4	49068.9	20070.2	44608.3	7398.1	35949.6	9198.1	35396.9
23757.1	49160.3	21981.3	44736.5	7450.1	36453.1	9501.3	36291.5
24195.6	49644.7	22437.8	44739.9	7656.2	37017.9	9541.6	37071.3
25339	72305.6	23852.8	63501.1	7727.7	37116.9	9827.3	37748.4
13864.5	72747.5	8941.7	64289.6	8527.9	37327.6	9908.5	37859.8
15007.9	73382	10444.6	64849	8615.6	37833.7	10715.8	38343.5
19821.2	73938.3	17476.8	65421.6	14165.1	47333.6	10945.9	41200.6
20076.6	74156.5	17969.5	65828.8	15305.8	47820.2	11032.5	41775.1
20127.3		18052.6		16018.9	48302.5	17699.5	42407.0
20425.1		18398.9		16023.5	48665.1	18015.4	43882.4
21023.5		19272.3		20053.8	49314.0	18416.6	44798.7
21130.2		19543.9		20169.5	49612.1	18721.4	45025.5
25484.5		22226.4		20568.2	50002.5	19571.3	45122.9
25860		22430.8		20827.4	72631.9	19833.5	63784.1
26154.1		22814.3		21422.9	73100.9	20370.3	64571.7
26355.7		25835.1		21585.1	73733.1	20423.7	65153.6
28970.3		27685		23878.6	74238.3	21668.9	65686.1
29301.2		27958		23941.8	74626.9	21924.4	66213.3
29918.4		29169.6		24306.4		22182.6	
30087.2		29240.6		24462.9		22486.3	
30226.7		29358.7		25281.2		22701.9	
30803.4		30286.2		25563.3		23174.0	
32241.9		31496.8		25690.7		23445.6	
32593.8		31956.6		26487.6		24252.1	
35263.4		34717.7		26731.5		24389.7	
35458		34764.4		27144.6		26156.1	
35676.6		35046.9		29309.5		27953.1	
36145.1		35945.2		29722.7		28328.3	
36281.5		36610		30248.3		29426.3	
36774.8		37549.2		30412.1		29507.0	

**Table S10.** CASSCF (7,5) + NEVPT2 computed Spin – Hamiltonian parameter (g, D, |E/D|) along with listed state – by – state contribution to the D values for both centre Co@1 and Co@2 in complex 1.

Parameters		Co@1		Co@2	
		CASSCF	NEVPT2	CASSCF	NEVPT2
		Contribution to D (cm <sup>-1</sup> )		Contribution to D (cm <sup>-1</sup> )	
D	EHA	77.9080	61.5835	75.1674	59.1513
E/D	EHA	0.2913	0.2805	0.3010	0.2984
<i>Effective g-values</i>					
	g <sub>xx</sub>	1.9848	2.0052	1.993030	2.011620
	g <sub>yy</sub>	2.3534	2.3508	2.352507	2.340117
	g <sub>zz</sub>	2.8997	2.7842	2.894520	2.779169
<i>g-values associated with KD1 (pseudo-spin ½)</i>					
		KD1: 54.4%  3/2; ±1/2⟩ + 45.6%  3/2; ±3/2⟩		KD1: 57.0%  3/2; ±1/2⟩ + 42.9%  3/2; ±3/2⟩	
	g <sub>xx</sub>	1.926484	1.789826	1.865479	1.727455
	g <sub>yy</sub>	2.691001	2.727127	2.615113	2.592733
	g <sub>zz</sub>	7.493167	7.249139	7.546766	7.327828
<i>g-values associated with KD2 (pseudo-spin ½)</i>					
		KD2: 50.3%  3/2; ±3/2⟩ + 49.7%  3/2; ±1/2⟩		KD2: 53.7%  3/2; ±3/2⟩ + 46.3%  3/2; ±1/2⟩	
	g <sub>xx</sub>	2.050405	1.938382	2.117679	2.016168
	g <sub>yy</sub>	2.198837	2.034838	2.238469	2.140741
	g <sub>zz</sub>	5.243054	5.489859	5.269889	5.474189

*EHA: Effective Hamiltonian approach*

**Table S11:** NEVPT2 computed spin-Hamiltonian parameters along with experimental studies obtained from PHI fitting for Cobalt centres in Complex 1.

	D(cm <sup>-1</sup> )		E/D		Fit	g <sub>min</sub> , g <sub>mid</sub> , g <sub>max</sub>
	Fit	Cal	Fit	Cal		Cal
Co@1	82.6	61.6	0.13	0.28	2.512, 2.631, 2.102	1.789, 2.727, 7.249
Co@2		59.2		0.29		1.727, 2.592, 7.327

**Table S12.** AILFT-derived ligand field parameters computed at CASSCF (in parentheses) and NEVPT2 level of theory for both centre Co@1 and Co@2 in complex 1 along with free Co(II) ion. The values of *B*, *C*,  $\xi$  parameters are provided in units of cm<sup>-1</sup>.

Parameter	Free Co(II)	Co@1	Co@1	% reduction	
				Co@1	Co@2
$\xi$	530.3	522.1	519.7	1.55	1.99
<i>B</i>	1040.3	1005.1	1005.9	3.38	3.30
	(1251.9)	(1197.9)	(1198.0)	4.31	4.30
<i>C</i>	4160.1	3849.2	3848.3	7.47	7.49
	(4621.0)	(4440.7)	(4440.8)	3.90	3.89
<i>C/B</i>	3.999	3.830	3.826	4.23	4.33
	(3.691)	(3.707)	(3.707)	-0.43	-0.43

$$\% \text{ reduction} = 1 - \left( \frac{\text{complex}}{\text{free Co(II)}} \right) \times 100$$

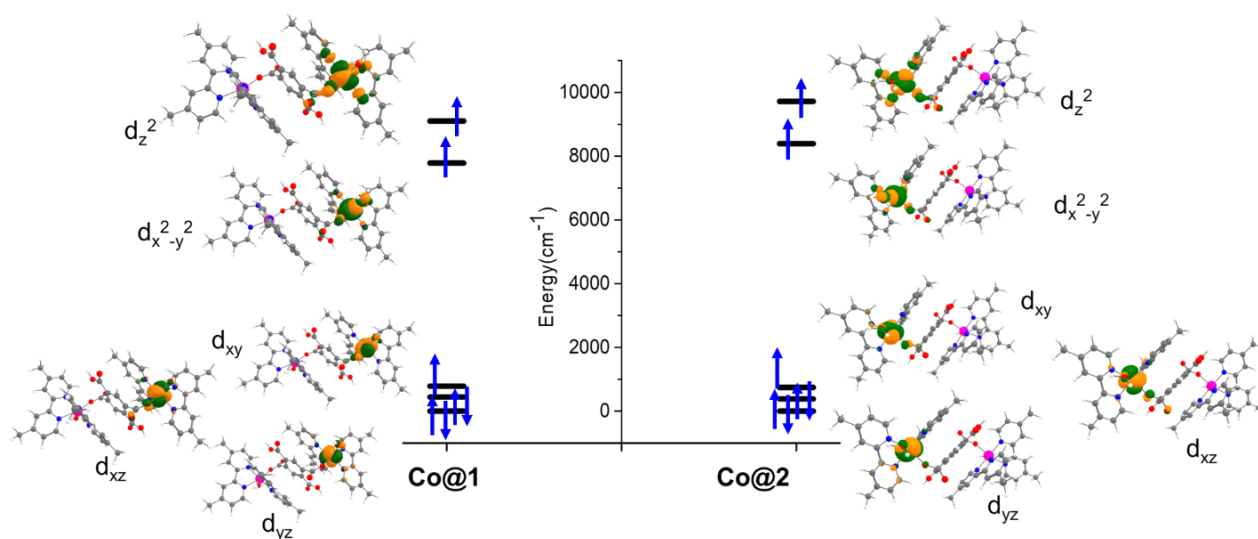


**Figure S15.** *Ab initio* ligand field theory (AILFT) computed d-orbital ordering for cobalt Co@1 (left) and Co@2 (right) in complex **1**. Color code: Co (cyan), N (blue), O (red), C (grey) and H (white).

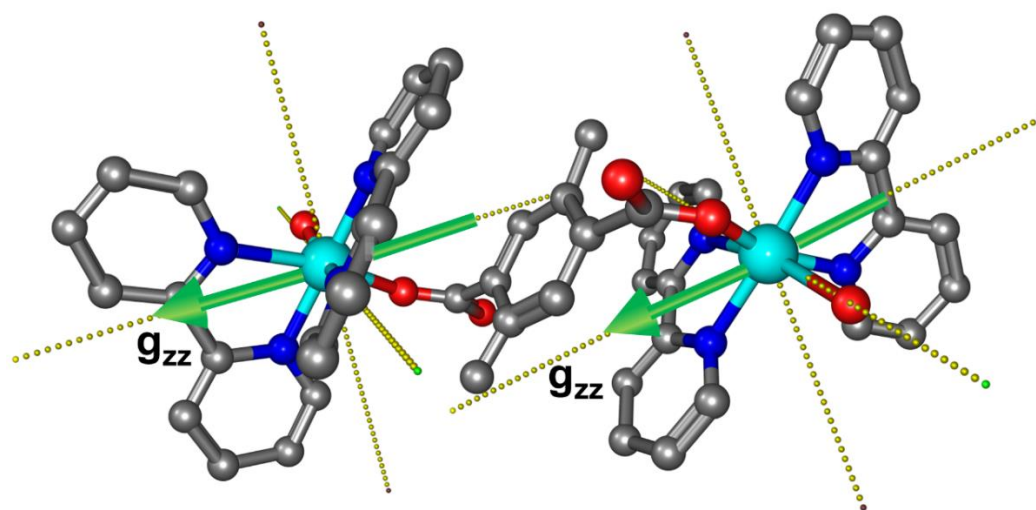


**Figure S16.** NEVPT2 computed  $g$ -tensor orientation in complex **1**. Color code: Co (cyan), N (blue), O (red), C (grey). Hydrogen atoms are omitted for clarity.



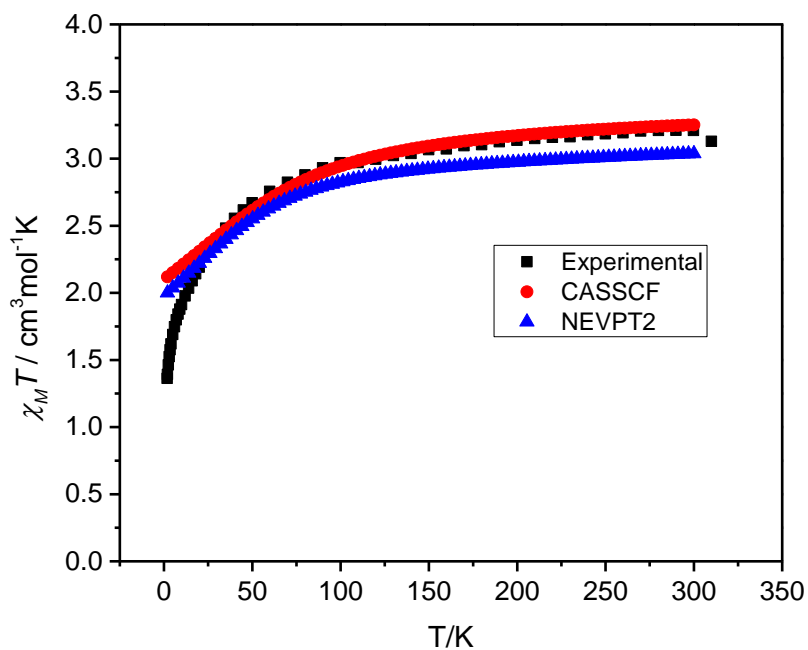


**Figure S17.** Experimental and ab initio computed magnetic susceptibility data of complex 1.

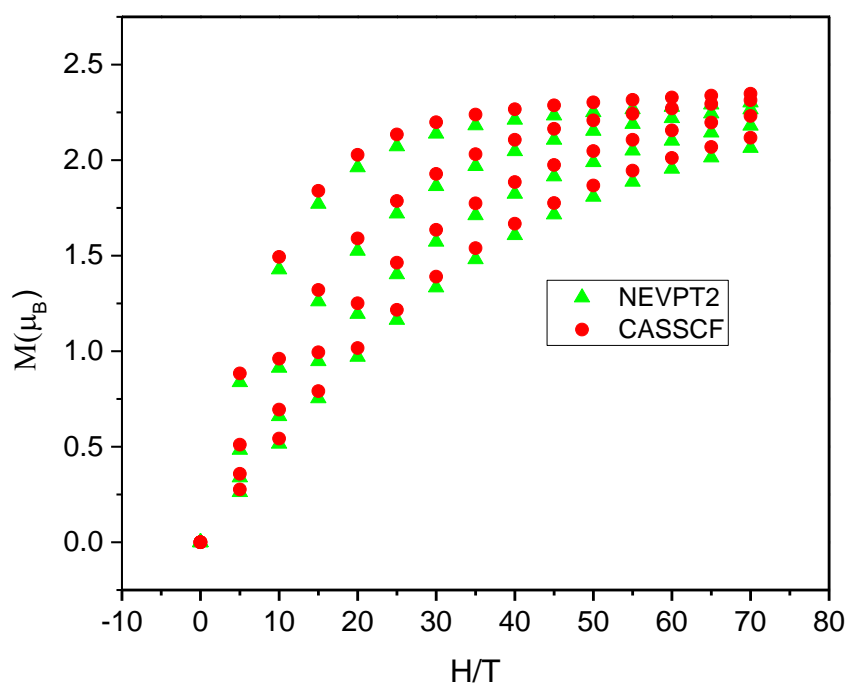


**Figure S18.** Ab initio computed magnetization curves for complex 1 at 2K, 3K and 5K.

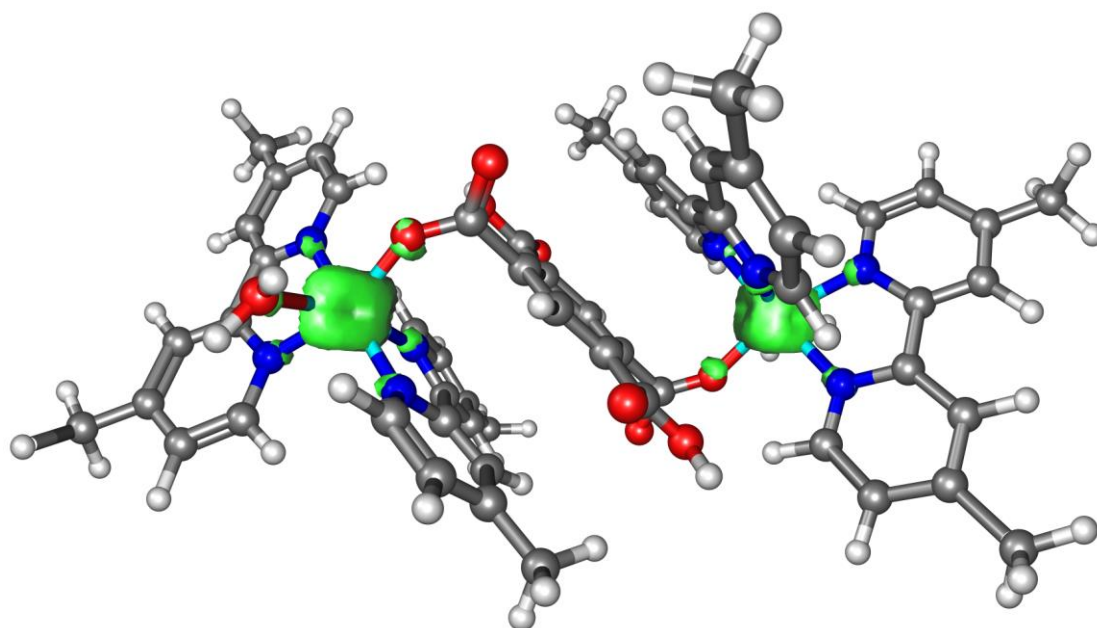


**Figure S19.** BS-DFT computed spin-density plot of ( $S=3$ ) ground state of **1**. The positive and negative spin densities are represented by purple and green colour, respectively. The iso-density surface represented here corresponds to a value of  $0.005410 e^- / \text{bohr}^3$ .

**Table S13.** BS-DFT computed energies of high-spin and broken-symmetry of complex **1** using  $H=-2JS_1S_2$  formalism.

Solution	Energy (Eh)	$\rho^{\text{Co1}}$	$\rho^{\text{Co2}}$	$\langle S^{*2} \rangle$	J( $\text{cm}^{-1}$ )
HS	-6221.869538	2.741111	2.740365	12.019750	0.02
BS	-6221.869537	2.741111	-2.740365	3.019865	

J values are estimated using the following equation,

$$J = -\frac{E_{HS} - E_{BS}}{S_{HS}^2 - S_{BS}^2}$$

**Computational Methodology: Periodic DFT**

The cell and geometry optimization of the X-ray structure of complex **2**, has been done using the first principal Density functional theory within the framework of periodic DFT on Vienna ab initio simulation package VASP<sup>5,6</sup>. The interactions between the electrons and ions have been accounted for using the projector-augmented-wave (PAW) method. The exchange-correlation functional generalized gradient approximation (GGA)/PerdewBurke-Eznerhof (PBE)<sup>7</sup> is used. The primary interaction playing role in this type of hybrid system is dispersion, hence this has been incorporated appropriately using the Grimme's DFT D3 dispersion<sup>8</sup> correction. Gamma-centred 1\*1\*1 K-point has been used for all calculations. The wave functions of the system contained in the supercell have been expanded in a plane-wave basis set with an energy cutoff of 520 eV. The structure optimization was continued until the maximum forces acting on each atom become less than 0.05 eV Å<sup>-1</sup>. The SCF convergence threshold was set to 10<sup>-6</sup> eV. Table S21 shows a comparison between the lattice parameters for complex **2** with the experimental structure. The optimized structure was used for further studying the electronic properties by doing Single Point using PBE functional and gamma-centered 2\*2\*2 K-Points along with a Hubbard correction parameter for Mn (U= 3.9 eV)<sup>9</sup> using DFT+U approach to get better results<sup>10</sup>. The Density of States calculations have also been performed at the same level.

**Table S14.** Comparison of the lattice parameters of complex **2** with the experimentally reported structure.

Experimental		Calculated	
a = 13.184Å	$\alpha = 90.0^\circ$	a = 13.264Å	$\alpha = 90.0^\circ$
b = 9.357Å	$\beta = 95.9^\circ$	b = 9.175Å	$\beta = 96.0^\circ$
c = 13.489Å	$\gamma = 90.0^\circ$	c = 13.319Å	$\gamma = 89.9^\circ$

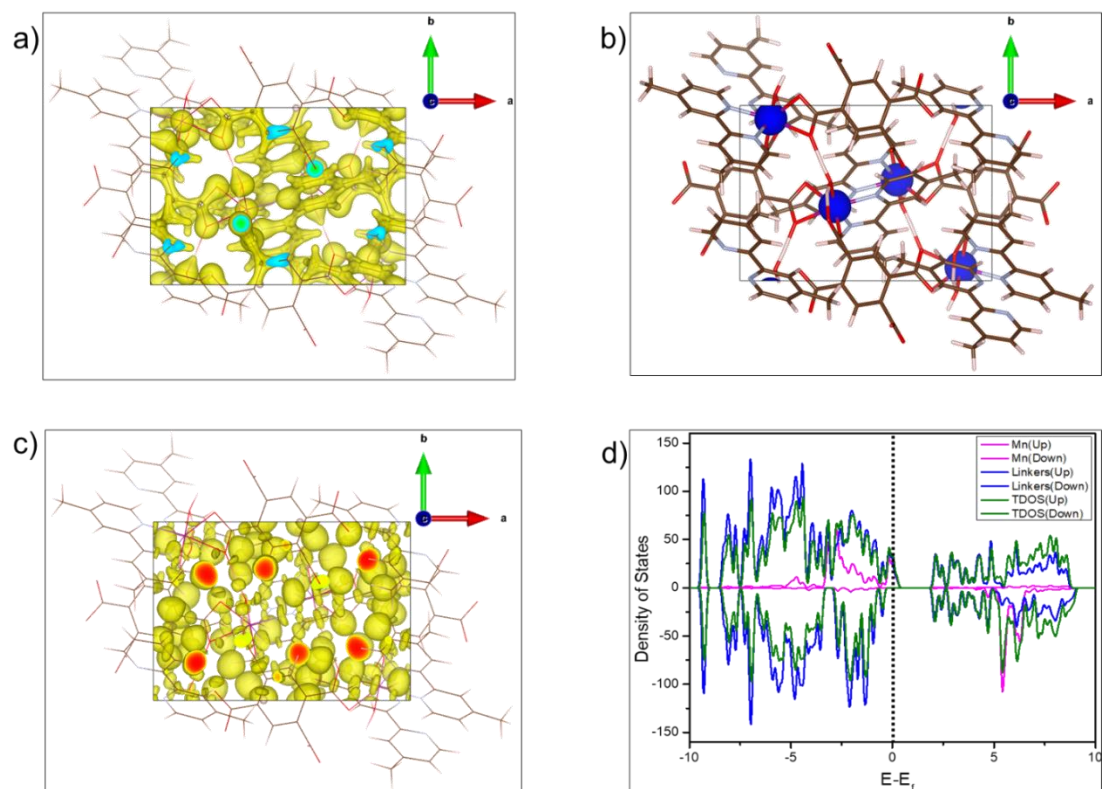


**Figure S20.** a) 1\*1\*1 supercell of complex **2** showing the Charge Density plot b) Spin density plot of complex **2** showing the electron density on each Mn(II) centres c) ELF plot for complex **2** d) Density of States plot for complex **2**.

**Table S15.** CASSCF (7,5) + NEVPT2 computed Spin – Hamiltonian parameter ( $g$ ,  $D$ ,  $|E/D|$ ) along with listed state – by – state contribution to the  $D$  value for Mn (II) center in complex **2m**.

Parameters		Mn	
		CASSCF	NEVPT2
		Contribution to $D$ ( $\text{cm}^{-1}$ )	
D	EHA	-0.0358	0.0497
$ E/D $	EHA	0.2554	0.2603
	$g_{xx}$	2.0021	2.0020
	$g_{yy}$	2.0021	2.0020
	$g_{zz}$	2.0021	2.0020
<i>g-values associated with KD1 (pseudo-spin <math>\frac{1}{2}</math>)</i>			
KD1: 47.5 % $\pm 1/2$ + 39.9 % $\pm 3/2$ + 11% $\pm 5/2$			
	$g_{xx}$	0.3814	0.8852
	$g_{yy}$	0.4956	1.3707
	$g_{zz}$	9.8378	9.4521
<i>g-values associated with KD2 (pseudo-spin <math>\frac{1}{2}</math>)</i>			
KD2: 47.8 % $\pm 5/2$ + 34 % $\pm 3/2$ + 24.6 % $\pm 1/2$			
	$g_{xx}$	3.8072	3.8428
	$g_{yy}$	4.1008	4.1159
	$g_{zz}$	4.7361	4.7078

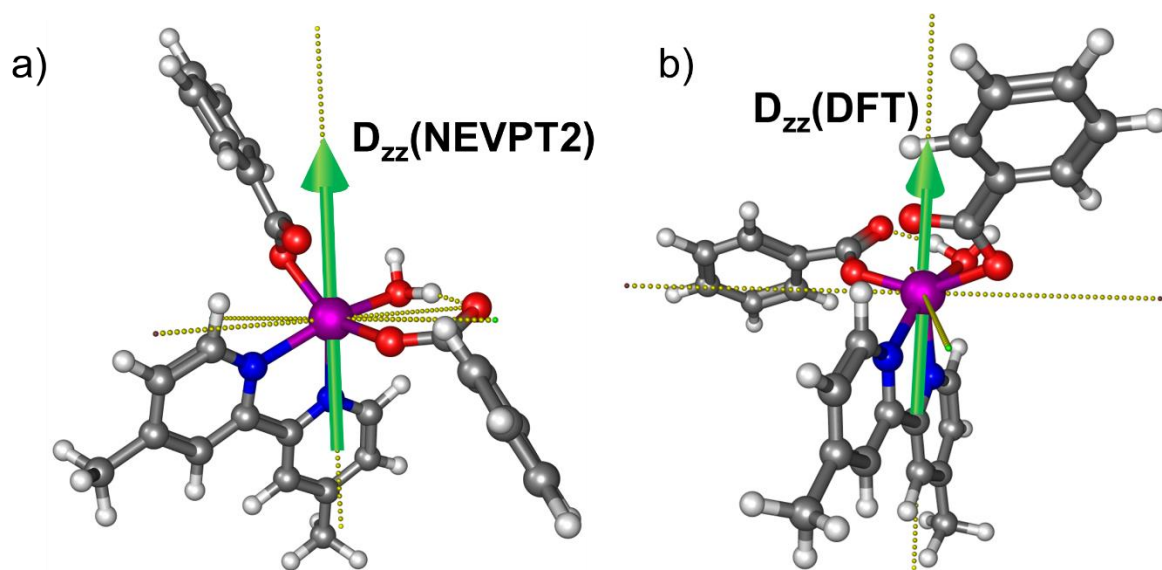


**Figure S21.** a) NEVPT2 computed D-tensor orientation and b) DFT computed D-tensor orientation in a mononuclear model complex **2m**. Color code: Mn (pink), N (blue), O (red), C (grey) and H (white).

**Table S16:** Comparison of NEVPT2 computed and DFT-PBE0 computed D values in complex **2m**.

Zero-Field Splitting	D (cm <sup>-1</sup> )
D (NEVPT2)	0.05
D (PBE0)	0.06
D <sub>ss</sub>	0.00044
D <sub>soc</sub>	0.06549
SOMO->VMO (alpha->alpha)	0.05912
DOMO->SOMO (beta ->beta )	0.05486
SOMO->SOMO (alpha->beta )	-0.02364
DOMO->VMO (beta ->alpha)	-0.02486



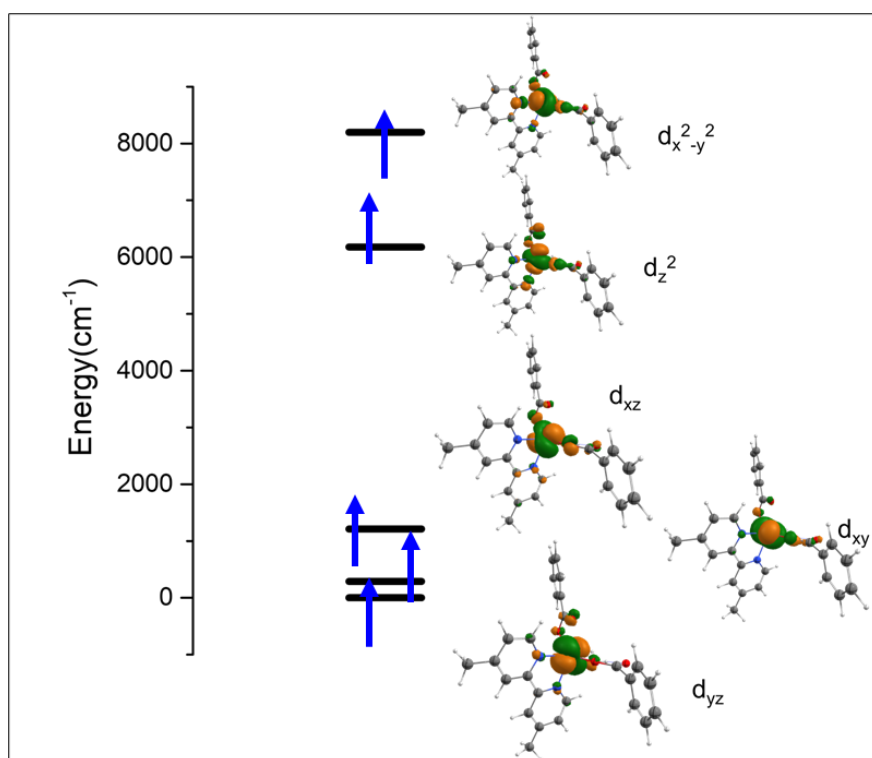


**Figure S22.** *Ab initio* ligand field theory (AILFT) computed d-orbital ordering for complex **2m**. Color code: Mn (pink), N (blue), O (red), C (grey) and H (white).

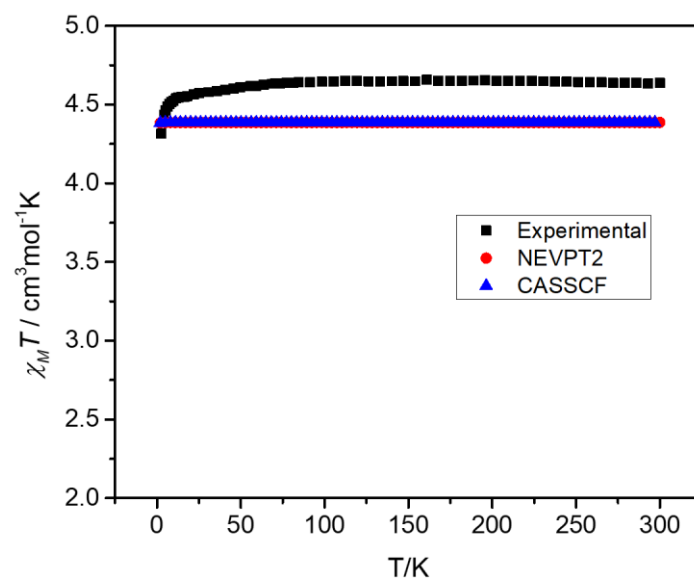


**Figure S23.** Experimental and Ab initio computed magnetic susceptibility plots for complex **2m**. The blue and red lines correspond to CASSCF and NEVPT2 computed data, respectively.

**Table S17.** CASSCF/NEVPT2 computed 1 spin-free sextet, 24 quartets and 75 doublets spin-free states along the spin-orbit states for Co centre1 in complex **2m**. All values are reported here in cm<sup>-1</sup>.

Mn							
SPIN-FREE STATES				SPIN-ORBIT STATES			
CASSCF		NEVPT2		CASSCF		NEVPT2	
0	58584.6	0	49707.7	0	51808.29	0	43698.34
25823.3	58763.4	19877	49918.8	0.13	52027.06	0.15	43900.29
26447	58915.8	20649.2	50047.2	0.24	52175.89	0.33	44109.33
27202.8	59169.5	21523.9	50244.6	25812.96	52258.88	19866.95	44142.71
29485.7	60679.6	24463.6	50598.5	25818.42	52513.66	19874.28	44199.86
29773.6	60930.2	24865.6	50620.7	26437.18	52571.1	20638.73	44303.15
29930.5	61138.2	25112.6	50628.7	26446.4	52782.81	20649.34	45659.48
30695.6	61254.7	26371.6	50927	27191.54	53290.48	21510.62	45723.76
30756.2	62244.1	26450.2	51461.9	27201.53	53407.76	21523.43	45773.29
30812	62814	26521.4	51807.3	29465.4	53617.59	24447.25	45827.98
36427.9	63232.7	29526.5	51881.2	29475.43	53749.1	24453.24	45877.66
36650.3	65251.7	29773.6	52161.5	29760.24	53874.8	24853.32	45979.67
37047.6	73866.8	30227.5	53280.5	29783.27	54205.5	24872.19	46332
38201.2	73990.2	31990.5	55315	29935.35	54359.82	25113.79	46414.07
38367.1	74452.2	32185.4	56577.3	29943.34	54509.47	25120.48	46931.94
38769.6	74755.3	33868.4	56971.6	30692.57	54691.41	26366.39	46995.45
39395.2	74861	34870.2	61755.9	30696.86	54738.43	26371.25	47360.22
40229.3	80294.9	35900.7	61880.7	30753.53	54908.9	26445.81	47442.16
51663	80656.2	43496.6	62406.4	30757.37	55238.46	26449.46	47776.34
51752.2	81304.7	43648.4	62832.4	30809.76	55522.19	26517.51	48072.04
52177.3	81444.6	44105.8	62998.5	30811.51	55909.64	26519.79	48110.41
52502.4	81709.5	44156.5	66476.7	36284.36	56699.83	27699.16	48180.22
53864.7	82186.1	46313.1	66935	36294.71	56928.33	28287.65	48290.31
54373.5	82300.5	46962.4	67908.2	36397.84	57086.73	29401.79	48438.98
54727.4	82409.6	47399.4	68093.4	36616.86	57672.05	29455.61	49746.71
36401.9	83030.7	69197.2	68460	36708.54	57795.49	29513.68	49958.61
36808.9	99301.4	69338.7	69197.2	36840.35	58136.53	29769.9	50083.78
37721.8	99376.3	28231	69338.7	37041.29	58315.98	29865.01	50309.75
39982	99503.8	29452.9	69495	37075.65	58634.16	30218.05	50575.69
40104.9	107686.9	33041.8	70199	37753.05	58787.46	30254.87	50691.7
40560.1	107769.5	33143.6	81186.5	38103	58971.8	31919.95	50727.42
40831.7	108026.3	33714.5	81270.7	38160.27	59252.75	31971.73	50996.14
41277.5	108195.8	33991.7	81368.5	38319.42	60708.51	32177.99	51503.65
41468.7	108337.5		89034.4				

41883.1	34644.2	89100.6	38379.18	60956.88	32222.68	51836.97
42541.5	34753.9	89459.1	38804.56	61165.01	33061.99	51931.44
42804.5	35323.6	89714.5	38867.47	61292.37	33149.43	52208.08
43798.5	36357.3	89835.5	39433.14	62258.09	33716.1	53307.7
46096.6	36816.6		39464.09	62811.43	33864.55	55343.08
46407.9	38296		40005.27	63402.25	33888.68	56556.68
46552.5	38997.9		40102.74	65269.91	34020.85	57123.31
46880.7	39112.4		40253.33	73889.36	34640	61784.55
47549.5	39440.5		40278.04	74014.13	34793.35	61910.96
49024.3	39480.2		40564.98	74466.64	34873.58	62430.12
49245.9	39578.7		40851.5	74763.01	34897.68	62848.66
49551.6	40615.9		41286.27	74915.16	35345.92	63048.66
51119.7	40892.5		41500.46	80313.57	35893.49	66501.54
51318.4	41237.6		41903.9	80672.94	35920.2	66958.54
52061	43036.8		42557.11	81317.56	36375.06	67928.11
52737.5	43214		42817.04	81470.4	36828.38	68123.31
53289	43934.1		43800.13	81737.19	38290.68	68491.03
53399	45714.1		46009.17	82210.39	38916.45	69225.5
53592.2	45760		46457.18	82325.54	39123.13	69367.65
53929.5	45784.9		46607.08	82435.24	39213.13	69524.4
54370	45795.4		46891.05	83053.16	39413.07	70225.06
54812.4	45864.1		47565.39	83053.16	39538.14	81178.25
55182	45946.7		49034.98	99289.13	39678.3	81293.58
55437.5	46147.1		49256.23	99398.57	40662.26	81393.74
55815.5	47812.8		49608.1	99523.67	40929.07	81902.18
56662	48018.1		51075.27	107709.3	41306.13	89130.71
56911.9	48029		51277.21	107793.2	42988.12	89486.63
57055.2	48061.1		51611.92	108047.9	43177.7	89745.3
57643.8	48222.3		51663.95	108223.7	43454.86	89877.78
57735.1	48378		51726.34	108376.1	43519.08	
58112.6					43612.38	
58259.8						

## References

- S1) SAINT Software Users Guide, version 7.0; Bruker Analytical X-Ray Systems: Madison, WI, 1999.
- S2) G. M. Sheldrick, SADABS, version 2.03; Bruker Analytical X-Ray Systems, Madison, WI, 2000.
- S3) G. M. Sheldrick, SHELXTL, Version 6.14, Bruker AXS, Inc.; Madison, WI 2000–2003.
- S4) O. V. Dolomanov, L. J. Bourhis, R. J. Gildea, J. A. K. Howard, H. Puschmann, OLEX2: A Complete Structure Solution, Refinement and Analysis Program. *J. Appl. Crystallogr.*, 2009, 42, 339–341.
- S5) G. Kresse and J. Furthmüller, *Phys. Rev. B*, 1996, 54, 11169–11186.
- S6) G. Kresse and J. Furthmüller, *Comput. Mater. Sci.*, 1996, 6, 15–50.

- S7) J. P. Perdew, K. Burke and M. Ernzerhof, *Phys. Rev. Lett.*, 1996, 77, 3865–3868.
- S8) S. Grimme, S. Ehrlich and L. Goerigk, *J. Comput. Chem.* 2011, 32, 1456–1465.
- S9) A. Mishra, T. Li, F. Li, EE. Santiso, *Chem. Mater.*, 2018, 31, 689-98.
- S10) P. Verma P, DG. Truhlar, *Theor. Chem. Acc.*, 2016,135, 182.